4420 *Biochemistry* **2010,** *49,* 4420–4431
DOI: 10.1021/bi100296z

BIOCHEMISTRY
including biophysical chemistry & molecular biology
Article

Core Histone Hyperacetylation Impacts Cooperative Behavior and High-Affinity Binding of Histone H1 to Chromatin†

Nikhil Raghuram,‡ Gustavo Carrero,§ Timothy J. Stasevich,∥ James G. McNally,∥ John Th'ng,⊥ and Michael J. Hendzel*,‡

‡*Department of Oncology, University of Alberta, 11560 University Avenue NW, Edmonton, Alberta, Canada T6G 1Z2,* §*Mathematics, Center for Science, Athabasca University, 10011-109 Street, Edmonton, Alberta, Canada T5J 3S8,* ∥*National Cancer Institute, National Institutes of Health, Bethesda, Maryland 20892, and* ⊥*Regional Cancer Centre, Thunder Bay Regional Health Sciences Centre, Medical Science Division, Northern Ontario School of Medicine, 955 Oliver Road, Thunder Bay, Ontario, Canada P7B 5E1*

Received February 28, 2010; Revised Manuscript Received April 11, 2010

ABSTRACT: Linker histones stabilize higher order chromatin structures and limit access to proteins involved in DNA-dependent processes. Core histone acetylation is thought to modulate H1 binding. In the current study, we employed kinetic modeling of H1 recovery curves obtained during fluorescence recovery after photobleaching (FRAP) experiments to determine the impact of core histone acetylation on the different variants of H1. Following brief treatments with histone deacetylase inhibitor, most variants showed no change in H1 dynamics. A change in mobility was detected only when longer treatments were used to induce high levels of histone acetylation. This hyperacetylation imparted marked changes in the dynamics of low-affinity H1 population, while conferring variant-specific changes in the mobility of H1 molecules that were strongly bound. Both the C-terminal domain (CTD) and globular domain were responsible for this differential response to TSA. Furthermore, we found that neither the CTD nor the globular domain, by themselves, undergoes a change in kinetics following hyperacetylation. This led us to conclude that hyperacetylation of core histones affects the cooperative nature of low-affinity H1 binding, with some variants undergoing a predicted decrease of almost 2 orders of magnitude.

Histone H1 or "linker histones" are of paramount importance in the formation and stabilization of higher order chromatin structure (*1*−*5*). There are at least six variants of histone H1 in mammalian somatic cells (H1.0, H1.1, H1.2, H1.3, H1.4, and H1.5) (*6*−*8*). These differ in their amino acid sequences, molecular weights, turnover rates (*9*), timing and pattern of expression (*10*, *11*), and efficiency of condensing DNA (*12*−*15*). The latter could be attributed to small but significant differences in the amino acid sequences of the C-terminal domain, which affects the DNA binding properties of each variant (*16*).

Positioned at the entry and exit points of DNA in the nucleosome, their highly basic C-termini interact with linker DNA to promote folding of the nucleosomal chain into highly organized chromatin fibers. Histone H1-containing nucleosomes constrain two left-handed superhelical turns comprising of 168 bp of DNA (*17*). A strong association of histone H1 with the nucleosome is thought to keep the DNA wrapped sufficiently tight to limit its accessibility to transcription factors and other nuclear proteins. This limited accessibility has implications for transcription, replication, recombination, and DNA repair (*18*).

Transcriptional activation is associated with changes to chromatin structure (*19*−*21*). Since histone H1 compacts DNA leading to limited nuclear dynamics, histone H1 was attributed the function of a global repressor of transcription (*22*−*25*). This assertion was countered by studies demonstrating that the influence of H1 on transcription is contingent upon the gene and may not always be repressive (*24*, *26*−*31*).

A more recent study showed that a 2-fold reduction in H1 levels in embryonic stem cells led to an at least 2-fold change in gene expression in only a few genes, although this impaired differentiation and resulted in death of mutant embryos in midgestation (*32*, *33*). Selective repression of genes has also been reported in histone H1 knockout mice (*32*, *33*). Linker histones have also been implicated in the precise positioning of nucleosomes (*27*), which may explain the selectivity of histone H1 in the regulation of specific genes.

The posttranslational modifications of histones by lysine acetylation is thought to reduce the binding of the histone H1 proteins to the nucleosome (*34*, *35*), leading to a more accessible chromatin structure (*36*, *37*). Genes in a transcription-competent state are characterized by increased core histone acetylation (*38*−*41*), whereas hypoacetylation is associated with gene silencing. Displacement of histone H1 by core histone acetylation not only alters chromatin condensation but may also regulate the activity of transcription factors and enzymes involved in DNA repair and recombination (*20*, *42*).

A steady state of histone acetylation is maintained by the antagonistic effects of two enzymes: histone acetyltransferases (HATs) (*42*) and histone deacetylases (HDACs) (*43*). Core histone acetylation occurs primarily at multiple highly conserved lysine residues and occurs in a site-specific manner (reviewed in ref *44*). Hyperacetylation of core histones prevents chromatin

†This work was supported by grants from the Alberta Cancer Research Institute and the Canadian Cancer Society Research Institute. M.J.H. is a senior scholar of the Alberta Heritage Foundation for Medical Research. G.C. has been supported by the Athabasca University Research Incentive Grant. N.R. is supported by the Endowed Graduate Studentship in Oncology and CIHR Graduate Studentship (Masters).

*To whom correspondence should be addressed. E-mail: mhendzel@ualberta.ca. Phone: 780-4328439. Fax: 780-4328892.

 Published on Web 04/23/2010

from folding into the 30 nm fiber and reduces the ability of chromatin to self-assemble into higher order structures (*45*, *46*). Recent work that substituted glutamine to mimic acetyllysine residues on core histones suggested that acetylation of H2B and H4 caused the greatest hindrance to nucleosomal self-association (*47*), switching between a relatively open state of chromatin and a closed one by reducing nucleosomal interactions and occluding the interactions between linker DNA and core histone tails (*44*). Acetylation of a single residue, lysine 16 of histone H4, could inhibit condensation of nucleosomal arrays in vitro (*48*), although the role that linker histones play in regulating this switch is not clear (*49*).

We have previously used FRAP[1] to establish the importance of the C-terminal domain of histone H1 in binding to chromatin (*50*). In addition, we have shown that the individual histone H1 subtypes vary considerably in their chromatin binding affinity (*16*) (reviewed in ref *51*). Mathematical modeling of FRAP recovery curves suggests that there are at least three different subpopulations of histone H1 in vivo, characterized as molecules bound with high affinity (which we will now term as HA sites), low-affinity (LA), and freely diffusing H1 molecules (*52*). In our current study, we have analyzed the influence of inhibition of HDACs by TSA on the mobility of N-terminal GFP-tagged constructs of all major somatic variants of H1 (H1.0−H1.5) as measured by FRAP. Contrary to previously published studies (*53*), we find that treatment with TSA for short durations (1−2 h) does not lead to significant change in H1 dynamics. The hyperacetylation of the core histones induced by lengthy (18 h) treatment with TSA induces a marked change in the binding of LA H1 molecules. Individual binding domains of H1 (CTD and globular domain), however, do not change their kinetics upon hyperacetylation. This leads us to conclude that hyperacetylation acts by decreasing the cooperativity with which H1 binds chromatin, thereby pushing the vast population of H1 molecules into a state that maintains a much less stable association with chromatin.

EXPERIMENTAL PROCEDURES

Cell Culture. Mouse embryonic fibroblasts (10T1/2 cells) and Ciras-3 cells (H-ras transformed 10T1/2 cells) were maintained in alpha-modified minimum essential media, supplemented with 10% fetal bovine serum and 1% L-glutamine. Cells were treated with trichostatin A (purchased from Sigma and dissolved in DMSO) at a concentration of 100 ng/mL for either 1 or 18 h.

Nuclei Isolation and Electrophoretic Separation of Histones. Nuclei were isolated as described in ref *54*, with some modifications. Briefly, 70−80% confluent cells were washed with ice-cold phosphate-buffered saline (PBS). Nuclei were isolated using ice-cold nuclear isolation buffer (250 mM sucrose, 150 mM NaCl, 20 mM Tris, pH 8, 2 mM $MgCl_2$, 1 mM $CaCl_2$, and 0.1% NP-40) supplemented with PhosSTOP (from Roche), a phosphatase inhibitor cocktail, pepstatin (Roche), DTT, and Complete protease inhibitor cocktail (Roche). Histones were extracted with 0.4 N sulfuric acid and precipitated with ice-cold acetone followed by centrifugation at 10000*g* for 10 min at 4 °C. They were then washed three times with acetone and stored at −20 °C until further analysis. Twenty micrograms of total histones was redissolved in acid−urea sample buffer and electrophoresed in acetic acid−urea−Triton X-100 (AUT) gels as described (*55*, *56*). Gels were then stained with Coomassie Brilliant blue.

For SDS gels, protein extracts were dissolved in SDS loading buffer (Tris−glycine−SDS), separated on a 18% acrylamide gel, and then transferred onto nitrocellulose membranes. Phosphorylated and total proteins were stained with Pro-Q Diamond Blot stains and SYPRO Ruby Protein Blot stain (Molecular Probes), respectively.

Antibodies against acetyllysine were purchased from Cell-Signaling Technology, mouse mAB 9681.

Fluorescence Recovery after Photobleaching. Mouse embryonic fibroblasts were cultured on number 1.5 glass coverslips in tissue culture media. They were then transfected with individual H1 variant constructs using Effectene (Qiagen) transfection reagent. Approximately 24 h after transfection, the binding affinity of histone H1 molecules was analyzed by FRAP. For global H1 analysis, a rectangular region (1.5 μm in length) was photobleached, encompassing both euchromatin and heterochromatin regions of the nucleus, and recovery was monitored at regular time intervals (*57*). Only the cells that expressed GFP-H1 at low concentrations were analyzed to avoid complications with H1 overexpression. For heterochromatin vs euchromatin H1 analysis, cells were pretreated with Hoechst 33342 (200 ng/mL) for 0.5 h and then replaced with fresh growth media. Hoechst itself did not have a statistically significant effect on H1 binding (Supporting Information Figure 1). Regions that stained intensely were the heterochromatin regions, while the remaining was classified as euchromatin. Two 1 μm diameter spots were simultaneously photobleached in heterochromatin and euchromatin regions, respectively. Images were corrected for cell movement and rotation using ImageJ software complemented with a specific algorithm plug-in (StackReg (*58*)). Intensity measurements were done with Metamorph software. Statistical tests for t_{50}/t_{90} and plotting of the FRAP curves were performed using GraphPad Prism version 5.00 for Windows, GraphPad Software, San Diego, CA.

Kinetic Modeling of H1 Dynamics in Vivo. A mathematical model was developed based on our previous studies (*52*, *57*), and the solution of the reaction-diffusion equation was fitted to those obtained from experimental FRAP data, allowing the estimation of multiple kinetic properties from a typical FRAP curve. The equations assume that histone H1 moves randomly throughout the nucleus and undergoes a reversible binding−unbinding interaction with chromatin. This analysis allowed an estimation of effective diffusion, binding and unbinding rates, and binding affinity. We also measured the proportion of the HA population and found an effective diffusion coefficient that accounts for a LA subpopulation and the freely diffusing subpopulation. These measurements were carried out for all cells subject to FRAP experiments. We then submitted the data to a two-sample Kolmogorov−Smirnov test (KS test) to determine if the set of estimated effective diffusion coefficients and binding affinities from the control groups differed significantly from those of the treatment groups. The reason for using nonparametric statistics for data analysis is the nonnormal distribution exhibited by the parameter distributions. Detailed mathematical equations, etc., can be found elsewhere (*52*, *59*).

RESULTS

Comparison of Binding Affinities among Different H1 Variants. Mathematical modeling revealed that histone H1 was

[1]Abbreviations: FRAP, fluorescence recovery after photobleaching; TSA, trichostatin A; GFP, green fluorescent protein; CTD, C-terminal domain; HA, high affinity; LA, low affinity.

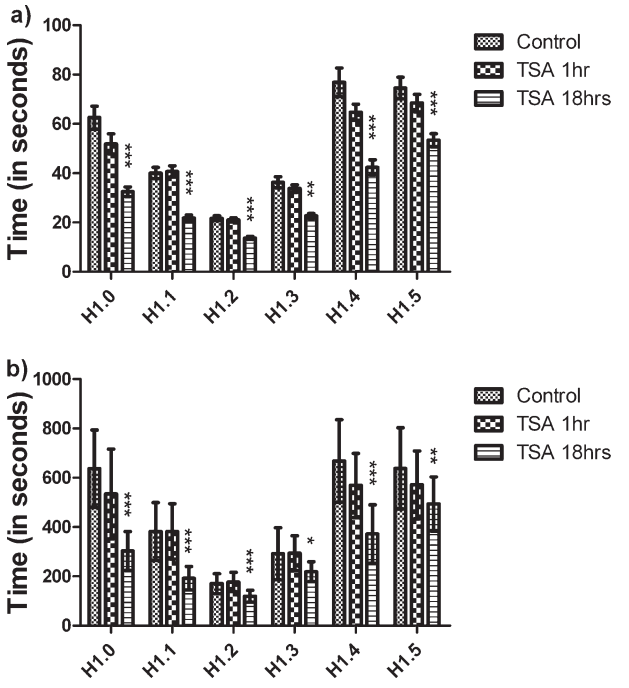

FIGURE 1: Comparison of t_{50} (a) and t_{90} (b) values of the six H1 variants before and after treatment with HDAC inhibitor, TSA. Based on the relatively high t_{50} and t_{90} values, we can group H1.0, H1.4, and H1.5 as a high-affinity H1 group, whereas H1.1 and H1.3 constitute a mid/medium-affinity group. H1.2 constitutes the low-affinity H1 group. Note that in H1.0, H1.4, and H1.5 there is a slight drop in t_{50} and t_{90} values after 1 h treatment although it was found to be insignificant. Major changes in these values were found only after 18 h of treatment with TSA. Each bar represents an average (±SEM) from 15 different FRAP experiments. Significance between control vs TSA (1 or 18 h) was analyzed using unpaired *t* test (95% confidence interval). [Notation for significance: (***) if *p* value is < 0.001, (**) if *p* is between 0.001 and 0.01, and (*) if *p* is between 0.01 and 0.05.]

not a single kinetic population. Rather, we obtained evidence for a HA (high-affinity) binding population and a second, larger population, with an effective diffusion coefficient that was several orders of magnitude too slow to be a diffusing molecule (*52*, *57*). Because most histone H1 is clearly, by direct visualization, associated with chromatin, we can conclude that this effective diffusion coefficient actually reflects a separate bound population, which we will refer to as LA (low affinity). For simplification, the time required for 50% recovery (t_{50}) is used as a surrogate marker for this population, which is the predominant form of histone H1 for every variant examined. We use a second measure, the time to 90% recovery, as a surrogate measure for changes in the smaller HA population. Note that the use of these surrogate markers is based on clear evidence obtained from mathematical modeling revealing that there are two distinct kinetic populations of the protein.

In order to characterize the changes in H1 dynamics in response to core histone acetylation, we studied the kinetics of H1 in cells with a basal level of core histone acetylation (control cells) compared with those containing hyperacetylated core histones. Previously, using SK-N-SH neuroblastoma cells, we showed that H1.1 and H1.2 had the weakest binding to chromatin whereas H1.4 and H1.5 bound strongly (*16*). Here, using 10T1/2 mouse embryonic fibroblast cells, we confirm a similar distribution (control cells in Figure 1). Based on the recovery profile of H1 variants in these cells, H1.2 had high rates of recovery and low t_{50} (21 ± 4 s) and t_{90} values (170 ± 40 s). H1.0, H1.4, and H1.5 behaved similarly and exhibited slow recovery kinetics, with a t_{50} of 62 ± 18, 76 ± 24, and 74 ± 18 s and t_{90} of 637 ± 156, 667 ± 168, and 638 ± 165 s, respectively. H1.1 and H1.3 had properties that reside between these two extremes. The t_{50} values in H1.1 and H1.3 were 40 ± 9 and 36 ± 11 s, respectively, while the t_{90} values were 382 ± 117 s in H1.1 to 292 ± 105 s in H1.3.

Changes in Histone Phosphorylation and Acetylation Post-TSA Treatment. To gain insight into the molecular dynamics of histone H1 in response to TSA treatment, we examined the acetylation and phosphorylation status of the core histones and H1 following such treatment. Mouse embryonic fibroblasts were treated with 100 ng/mL TSA for 0.5, 1, or 18 h. Cells were then harvested, and the isolated histones were analyzed using acetic acid−urea−Triton X-100 (AUT) gel electrophoresis (Supporting Information Figure 1a,b). Some increase in histone acetylation was detectable within the first 30 min of TSA treatment, as indicated by the relative increase of monoacetylated H4 and the corresponding decrease in unacetylated H4. After 1 h treatment with TSA, there is an increase in mono-, di-, and a small amount triacetylated H4 species. After 18 h of TSA treatment, mono-, di-, tri-, and tetraacetylated H4 species were abundant. Treatment of TSA for 48 h did not lead to a further appreciable increase in H4 acetylation (data not shown). Immunoblotting analysis using an antibody directed against acetyllysine was carried out to further characterize the changes in acetylation in core histones (Supporting Information Figure 1c,d). TSA treatment for 0.5 h increased overall acetylation levels in core histones by 1.4-fold, and a further increase to 2-fold (over control cells) was observed following 1 h treatment with TSA. After 18 h, there was a 7-fold increase in core histone acetylation over the untreated control cells. The antibody was unable to detect acetyllysine residues on histone H1 in either control or hyperacetylated cells (figure not shown).

TSA exerts cellular effects other than inhibition of HDAC, including an inhibition of proliferation through the induction of p21 WAF1/Cip1 (*60*), which inhibits the histone H1 kinase cdk2. This additional activity complicates the study on the impact on histone H1 binding, since phosphorylation of H1 has been shown to destabilize H1 binding and its inhibition would be expected to increase the binding affinity of histone H1. These secondary effects, which are characterized by induction of genes susceptible to changes in histone acetylation status, would be observed only after prolonged treatment with TSA (greater than 6 h). Consistent with that expectation, changes to the phosphorylation of H1 or that of core histone phosphorylation status were not observed with brief treatments with TSA. With prolonged treatment of 18 h, we found the levels of core histone phosphorylation to be similar to those observed in control cells. The level of H1 phosphorylation, however, was lower after 18 h of TSA treatment as compared to control cells (Supporting Information Figure 2a,b). Notably, the expression of H1.0 is also upregulated in these cells. Phosphorylated histones from the ras-transformed Ciras-3 mouse cells were included as a positive control, where phosphorylation is observed on histone H1, H2A, and H3 (data not shown).

Analysis of Histone H1 Dynamics Post Induction of Core Histone Acetylation (*TSA, 1 h*). Based on the above results, the most significant change in chromatin that we observe upon TSA treatment (1 h) is an upregulation of global histone acetylation levels. We proceeded to test the impact of TSA treatment on histone H1 binding using FRAP. MEFs were incubated with

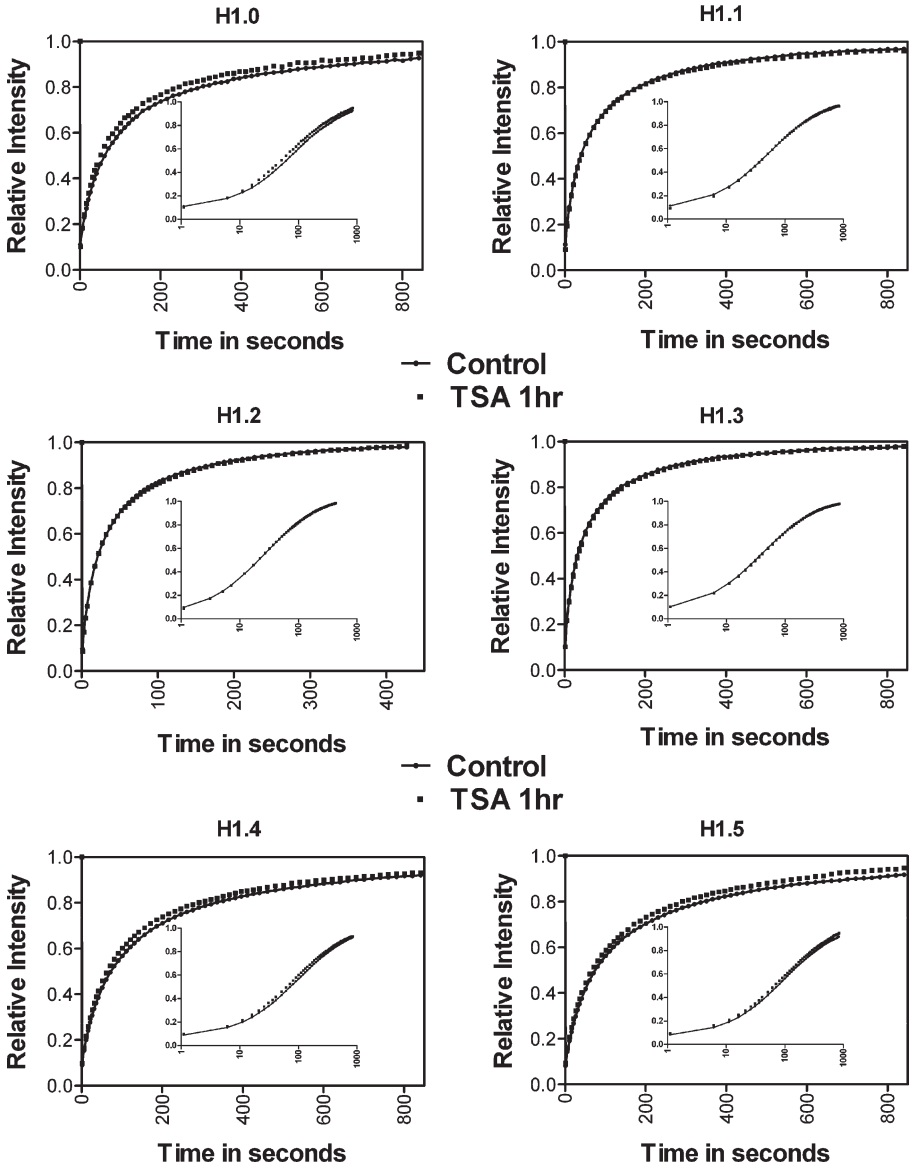

FIGURE 2: FRAP recovery profiles postinduction of core histone acetylation (TSA treatment for 1 h). Each FRAP recovery curve shown here is an average from 15 different FRAP experiments, repeated at least three times. The plots show the relative intensity versus time (in seconds) for each of the six H1 subtypes. The inset replots the recovery profiles as the relative intensity versus the log of time. This better illustrates the recovery at earlier time points (1−100 s). Note that in most variants there is no change in recovery profiles following 1 h TSA treatment.

TSA for 1 h and were then subjected to FRAP experiments. The results show that a brief treatment with histone deacetylase inhibitors does not lead to any significant increase or decrease in histone H1 binding. All variants fail to show a change that reaches statistical significance (Figures 1 and 2).

While t_{50} and t_{90} can provide some information on the changes in LA and HA binding sites, they are not as informative as extracted kinetic information obtained from mathematical modeling. Using the latter approach, we are able to obtain information on changes in pool sizes, the amount of time H1 molecules spend bound to the chromatin (residence time (res T)), and the amount of time spent in the weakly bound and freely diffusing states before engaging in a high-affinity binding event (transition time (T trans)). Changes in the effective diffusion coefficient provide a measure of binding to LA sites (*52*, *61*). Specifically, increased effective diffusion rates require that the binding to LA sites be reduced in duration and/or that there be fewer LA sites available for binding, resulting in an increased freely diffusing pool.

Consistent with the trend seen in t_{50} and t_{90} values, no change in any kinetic parameter proved to be statistically significant following treatment with TSA for 1 h (Table 1).

Histone H1 Dynamics with Hyperacetylated Core Histones. To investigate the effects of core histone hyperacetylation on H1 mobility, we performed FRAP analysis after treating cells with TSA for 18 h (overnight incubation) (Figure 3).

H1.1 and H1.2 revealed a statistically significant drop in t_{50} and t_{90} values ($p < 0.001$) (Figure 1). This suggests that both the loosely bound subpopulation, which predominates in the t_{50} measurement, and the strongly bound subpopulation, reflected in the t_{90} measurement, were altered by core histone hyperacetylation. Both subtypes share a similar FRAP recovery profile: the two curves (control and TSA, 18 h) converged at later time points. Histone H1.3 showed modest changes in mobility following core histone hyperacetylation. The t_{50} and t_{90} revealed a statistically significant decrease, although the drop in t_{90} was not as dramatic as seen in other variants. The strongly binding H1 variants, H1.0, H1.4, and H1.5, were also affected by the

Table 1: Detailed Kinetic Modeling Data[a]

H1 variant		control				TSA, 1 h				TSA, 18 h			
		D_{eff} (μ^2/s)	B (%)	res T (s)	T trans (s)	D_{eff} (μ^2/s)	B (%)	res T (s)	T trans (s)	D_{eff} (μ^2/s)	B (%)	res T (s)	T trans (s)
H1.0	median	0.008	20	624	2498.5	0.009	20	606	2043	0.013	16	346	2189
	p-value					0.65	0.86	0.59	0.54	0.004	0.54	0.01	0.34
H1.1	median	0.01	19	349	1406.5	0.009	18	439	2376	0.02	18	149	659.8
	p-value					0.35	0.10	0.35	0.35	0.001	0.51	0.01	0.05
H1.2	median	0.016	18	157	787.35	0.017	16	179	1070	0.024	13	141	980.8
	p-value					0.46	0.84	0.46	0.12	0.001	0.03	0.19	0.19
H1.3	median	0.01	18	330	1422.5	0.011	16	312	1559	0.017	18	219	956.3
	p-value					0.28	0.23	0.72	0.95	0.001	0.62	0.03	0.10
H1.4	median	0.005	19	716	2967.3	0.006	19	661	3278	0.009	19	392	1875
	p-value					0.14	0.71	0.93	0.94	0.001	0.48	0.04	0.24
H1.5	median	0.005	17	667	3170.7	0.006	21	518	1549	0.008	22	502	1919
	p-value					0.18	0.16	0.13	0.12	0.01	0.27	0.10	0.04

[a]Kinetic parameters were obtained after modeling each FRAP curve based on the model described in Carrero et al. The effective diffusion coefficient is associated with the freely diffusing and low-affinity population, while residence time is an indicator of the affinity of the strongly bound population. The level of significance was determined by a two-sample Kolmogorov−Smirnov test.

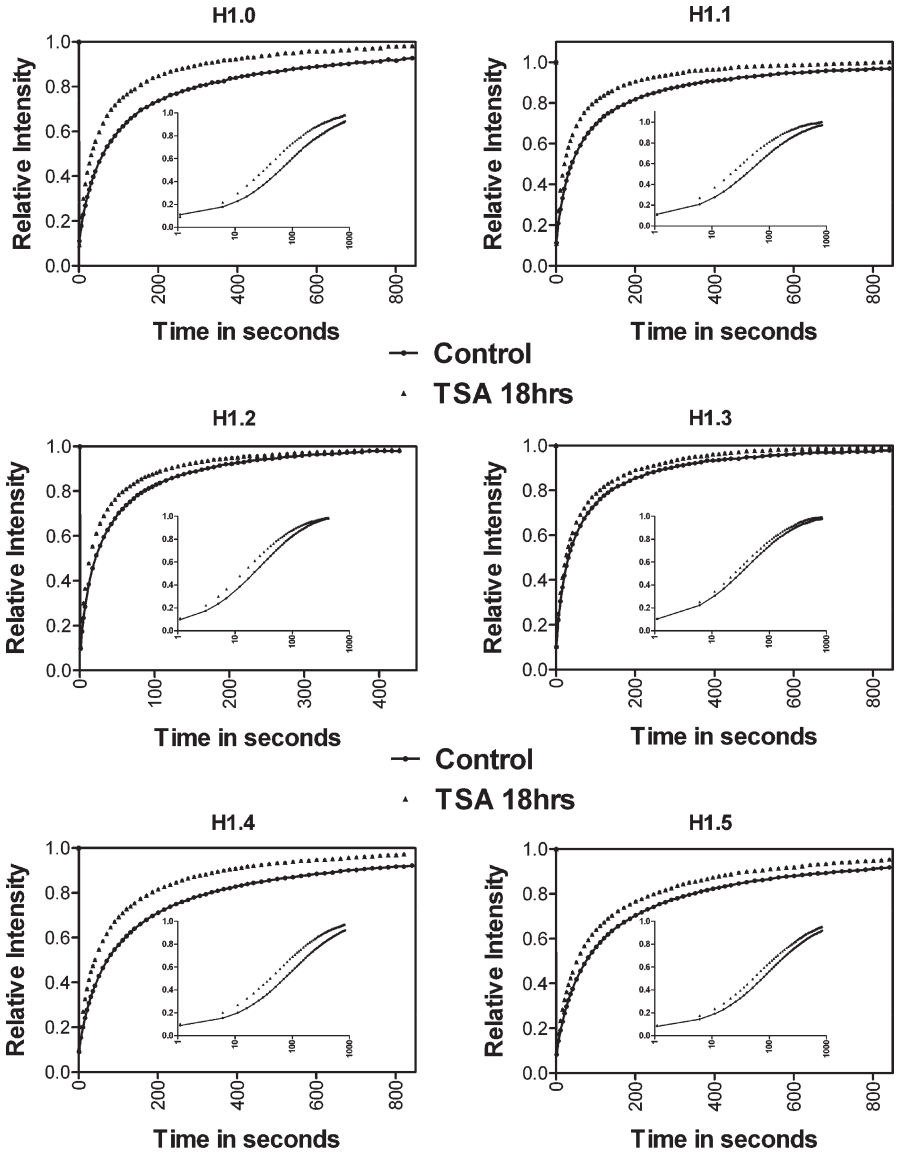

FIGURE 3: FRAP recovery profiles postinduction of core histone hyperacetylation (TSA treatment for 18 h). Each FRAP recovery curve shown here is an average from 15 different FRAP experiments, repeated at least three times. The plots show the relative intensity versus time (in seconds) for each of the six H1 subtypes. The inset replots the recovery profiles as the relative intensity versus the log of time. Note that in most variants there is a marked change in recovery following core histone hyperacetylation. This is most prominently seen in H1.0, H1.1, H1.4, and H1.5.

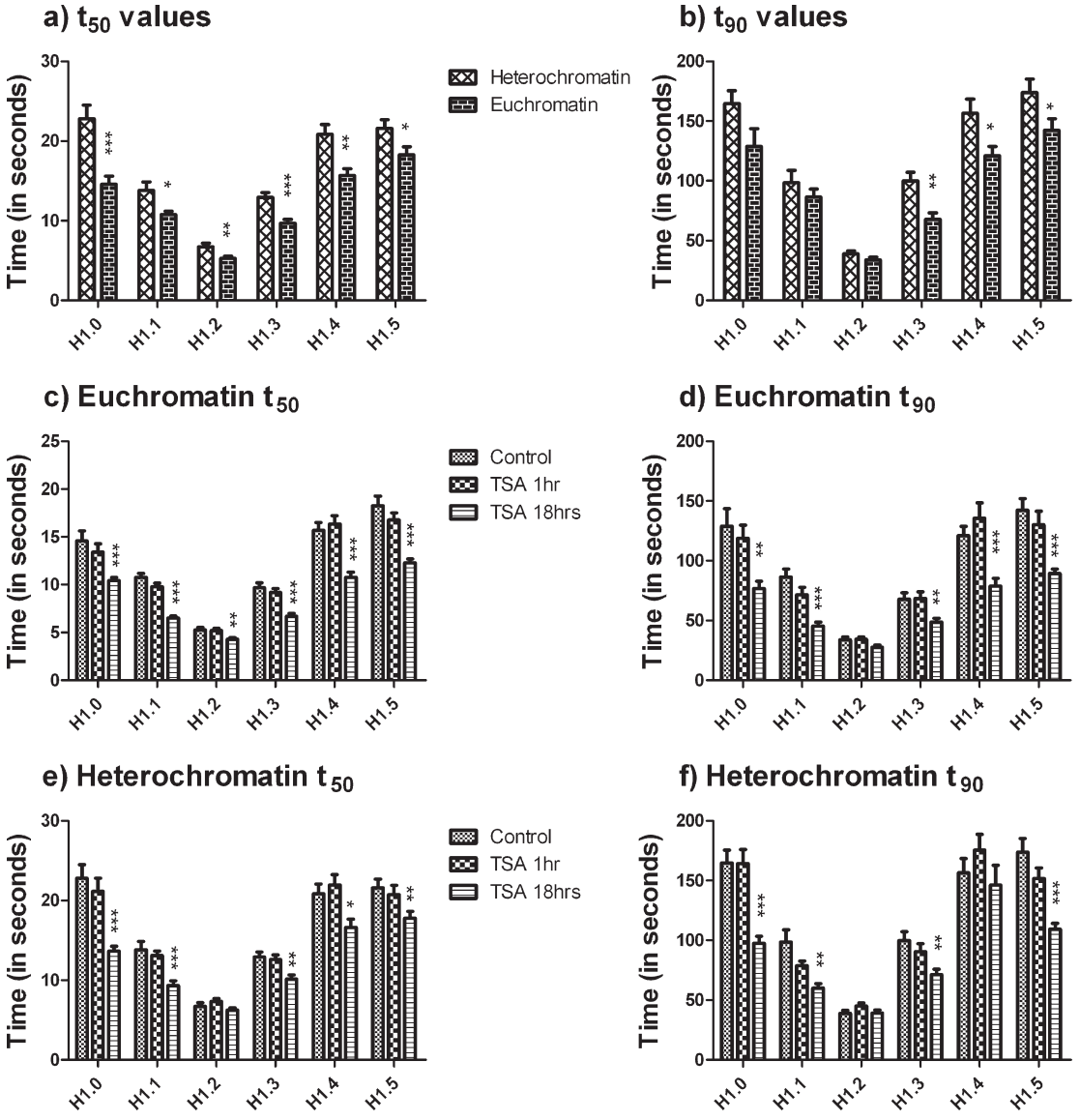

FIGURE 4: Comparison of t_{50} and t_{90} values between heterochromatin- and euchromatin-enriched H1 variants. Panel a represents the t_{50} values obtained from the FRAP recovery profiles of the different variants following a spot bleach that specifically targeted either euchromatin or heterochromatin regions (ascertained via staining with Hoechst 33342). Panel b represents the t_{90} values from the same. Panels c and d represent the t_{50} and t_{90} values following spot bleach in euchromatin regions, respectively, after 1 and 18 h TSA treatment. Panels e and f represent the t_{50} and t_{90} values following spot bleach in heterochromatin regions of the nucleus, after 1 and 18 h TSA treatment. Each bar represents an average (±SEM) from 15 different FRAP experiments. Significance between control vs TSA (1 or 18 h) was analyzed using unpaired t test (95% confidence interval). [Notation for significance: (***) if p value is < 0.001, (**) if p is between 0.001 and 0.01, and (*) if p is between 0.01 and 0.05.]

18 h TSA treatment. There was a statistically significant ($p < 0.001$) drop in the t_{50} values in all three variants, suggesting that the loosely bound subpopulation increases its mobility upon TSA treatment. H1.0, H1.4, and H1.5 show a concomitant statistically significant drop in t_{90} values as well ($p < 0.001$ in H1.0 and H1.4 and $p = 0.003$ in H1.5). Interestingly, there is less apparent convergence in the recovery curves from control and TSA-treated cells for these more tightly binding histone H1 subtypes.

We then proceeded to mathematically model the FRAP curves enabling us to better understand the changes in kinetic behavior of H1 molecules postinduction of core histone hyperacetylation. The hyperacetylation observed after an 18 h treatment with TSA led to significant changes in the kinetic parameters, although the changes were not uniform among all variants (detailed information can be found in Table 1). The results of kinetic modeling show that there are significant increases in the effective diffusion coefficient in all variants analyzed (a p-value of less than 0.001 in H1.1, H1.2, H1.3, and H1.4, 0.004 in H1.0, and 0.01 in H1.5).

The changes to the HA population were variant dependent. With the exception of histone H1.2, there was no statistically significant change in the proportion of H1 at HA sites after 18 h of TSA treatment ($p = 0.03$). Although the proportion did not change in most variants, the residence time dropped significantly in H1.0, H1.1, H1.3, and H1.4 (1.5−2-fold decrease compared to control cells). A decrease in residence time indicates a decrease in affinity to the HA sites and is inversely proportional to the dissociation rate of HA molecules to the freely diffusing/LA states.

Another similar time-dependent parameter obtained is the time H1 molecules spend cycling back and forth between the freely diffusing population and LA state before converting to a HA stably bound H1 population. This is known as the transition

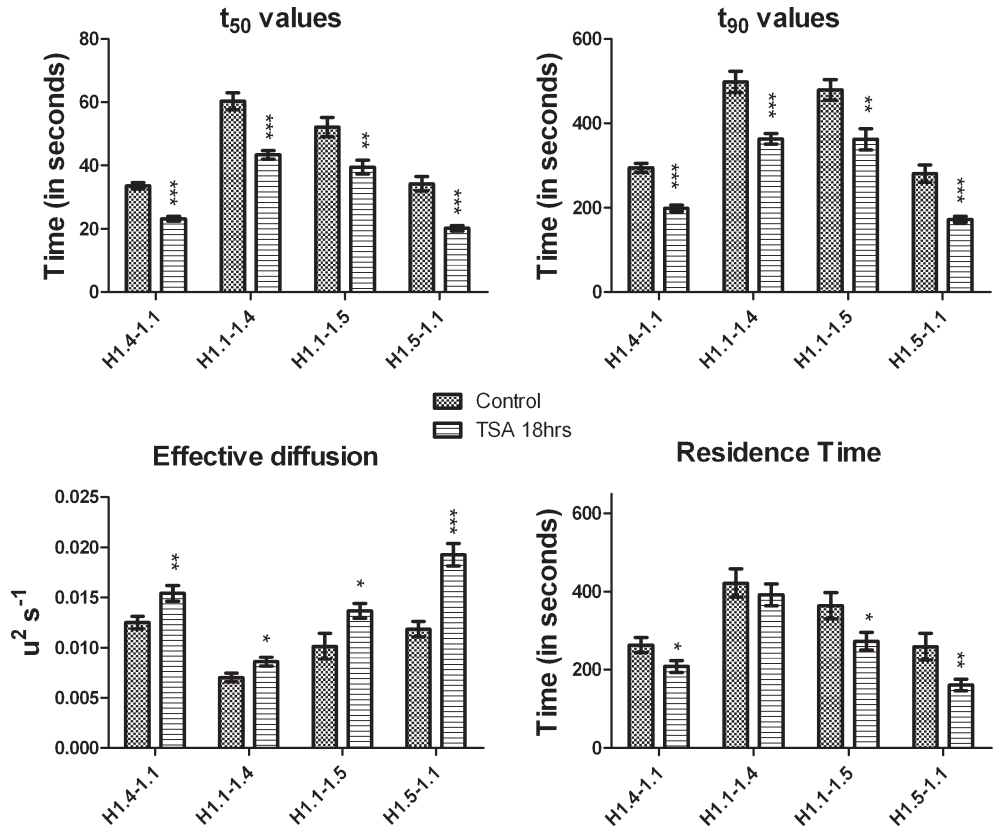

FIGURE 5: Comparison of t_{50}, t_{90}, and kinetic parameters of H1 hybrids following core histone hyperacetylation (TSA, 18 h). All of the hybrids showed a drop in t_{50}, t_{90}, and D_{eff} values, similar to the response seen in their "parent" H1 subtypes. The change in residence time, however, varied.

time, and the higher the transition time, the lower the association rate of HA H1 molecules. The only H1 variants in which a change in this parameter was observed were H1.1 and H1.5 ($p = 0.049$ in H1.1 and $p = 0.044$ in H1.5).

Heterochromatin vs Euchromatin. Several studies have shown that specific H1 variants have preferential localization within the nucleus, some showing greater enrichment in euchromatin, while others in heterochromatin (*16*, *62*). Using GFP-tagged H1 variants and Hoechst staining, we had previously shown that in MEF's H1.0, H1.1, H1.2, and H1.3 had a preferential enrichment in euchromatin, while H1.4 and H1.5 showed greater enrichment in heterochromatin (*16*). A similar pattern was found in human fetal fibroblasts using immunoprecipitation experiments (*63*).

To quantify the changes in recovery patterns in these subdomains upon treatment with TSA, we photobleached a spot of 1 μm in diameter, specifically targeted to regions that were densely stained with Hoechst (heterochromatin) and those that were not (euchromatin). The mouse embryonic fibroblasts show visually distinct heterochromatin and euchromatin regions (*16*). Hoechst did not affect the binding of H1 at the concentrations used in this study (Supporting Information Figure 3).

(*a*) *Control Cells*. Statistically significant differences in t_{50} were found between heterochromatin- and euchromatin-enriched pools for each variant, with the euchromatin-enriched H1 molecules recovering much faster (lower t_{50}) than those enriched in heterochromatin (Figure 4a). Similar changes were observed in t_{90} values, although the change in mobility between heterochromatin and euchromatin is most distinct in H1.3, H1.4, and H1.5 (Figure 4b). The significant changes seen in the t_{50} value for all variants suggest that the major contributor to the kinetic disparities between heterochromatin- and euchromatin-enriched H1 molecules stems from the low-affinity subpopulation of linker histones. Only histones H1.3, H1.4, and H1.5 showed a statistically significant difference in the t_{90} value, suggesting a physical difference in the HA sites for these histones in euchromatin versus heterochromatin.

(*b*) *Induction of Hyperacetylation*. To analyze the effect of core histone acetylation and hyperacetylation on the binding of H1 population between the euchromatin and heterochromatin, we treated MEF cells with TSA for 1 and 18 h, respectively, and then specifically measured the recovery rates in the euchromatin and heterochromatin regions. Similar to the results in Figure 1, the 1 h TSA treatment did not cause any statistically significant changes in t_{50} or t_{90} values for all variants (Figure 4c−f; FRAP curves are shown in Supporting Information Figures 4−7). However, the values were reduced in a manner that is consistent with the trend previously observed after 18 h of treatment.

Following treatment with TSA for 18 h, statistically significant decreases in t_{50} in the euchromatin pool were observed for all of the H1 variants (Figure 4c,d). When the time was represented in the log scale, significant changes seen in the low-affinity H1 population were obvious (Supporting Information Figure 4). In heterochromatin-enriched pools of H1, however, there were also differences in the FRAP recovery profiles. A statistically significant drop in t_{50} was observed for all of the variants, except for H1.2 (Figure 4e,f). The decline, however, was not as prominent as that seen in euchromatin. The t_{90} measurements showed that not all variants responded to the 18 h TSA treatment according to their affinities. The t_{90} values of the low-affinity H1.2 and high-affinity H1.4 were not affected by the TSA. The absence of an

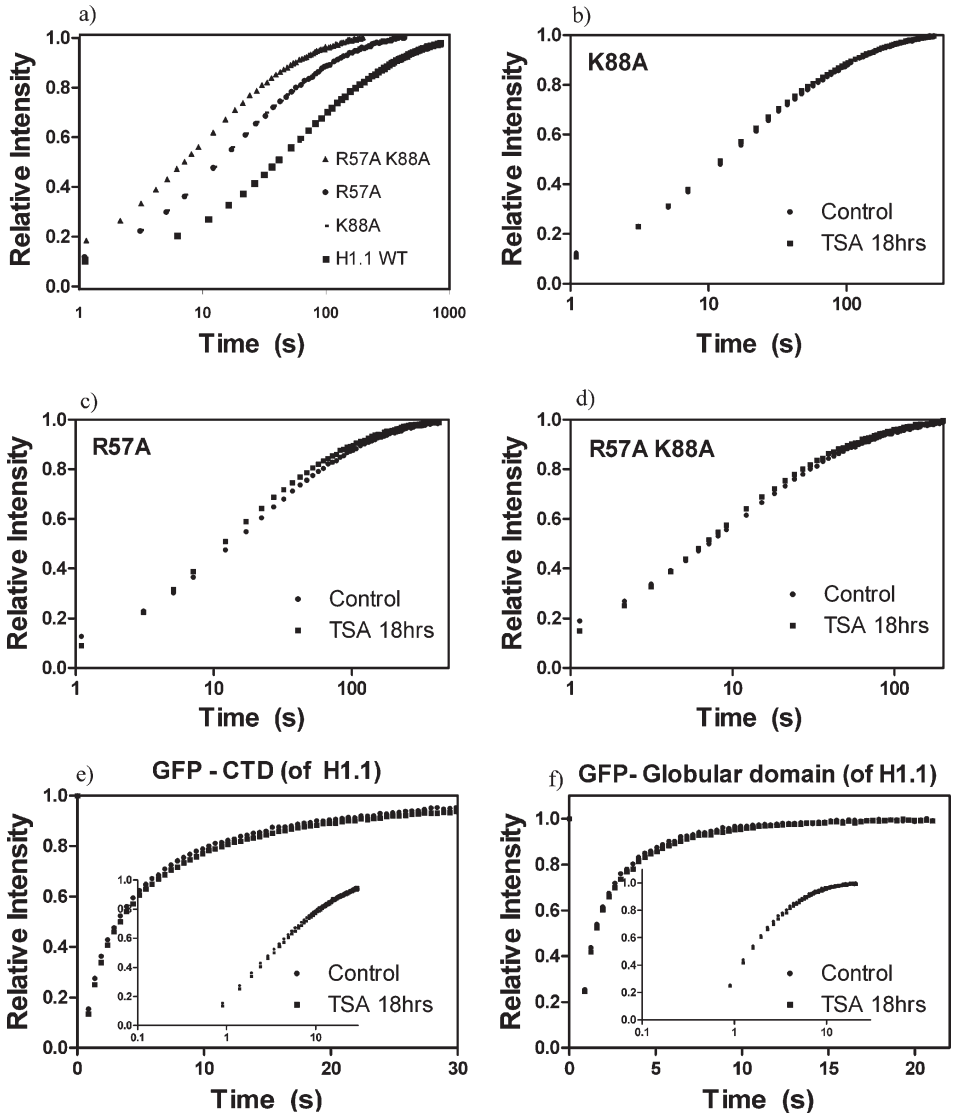

FIGURE 6: Behavior of individual domains of H1 to hyperacetylation. (a) Key residues within the globular domain (site I, site II, or both) were mutated, and their recovery was monitored with FRAP. This is a comparison in untreated cells (basal levels of acetylation). (b−d) FRAP recovery curves of the mutants following an induction of hyperacetylation. Note that mutation of just one residue in the globular domain can entirely abrogate the kinetic response to hyperacetylation. (e, f) Both the globular domain and the CTD (of H1.1) by themselves fail to show a change in recovery following hyperacetylation.

effect in the H1.2 was also seen in the t_{50} measurements, but the heterochromatin-enriched H1.4 showed an initial decline in t_{50} values. Similar to H1.0, the other heterochromatin-enriched variant, H1.5, showed a steep decline in t_{90} value. H1.0, H1.1, and H1.5 display a trend that is very similar to the population enriched in euchromatin.

H1 Hybrids and Their Response to Hyperacetylation. Both the globular domain and the CTD have been shown to have an impact on H1 binding, with the CTD being the primary determinant for HA binding (*50*, *64*). In order to understand which domain of H1 played a role in influencing the behavior of H1 variants toward core histone hyperacetylation, we constructed H1 hybrids, which have the CTD and globular domain swapped between different variants (*16*). For example, H1.1−1.4 has the globular domain of H1.1 and the CTD of H1.4. Should the CTD be the primary determinant that influences the changes seen upon core histone hyperacetylation, then all hybrids that harbor the same CTD should give a similar kinetic response. Since the globular domain is identical in H1.1−H1.5, the only other difference between the variants is restricted to the short amino-terminal domain (NTD). Differences between the behavior of the CTD in the native histone versus the hybrid, then, would imply a role for the NTD in the acetylation response.

In all of the H1 hybrids analyzed (H1.1−1.4, H1.4−1.1, H1.5−1.1, H1.1−1.5), we observed a decrease in t_{50} and t_{90} values, consistent with those observed for their "parent" molecules (Figure 5). There was a consistent decrease in effective diffusion coefficient upon core histone hyperacetylation in all of the hybrids. Hybrids H1.4−1.1 and H1.5−1.1, which share the same CTD of H1.1, also share a similar kinetic response seen in native H1.1, with a decrease in residence time and a stable proportion of strongly bound molecules being maintained. The change in the HA kinetic parameters, however, cannot be entirely explained by the sequence of the CTD. Hybrid H1.1−1.4, which shares the CTD of H1.4, did maintain a stable pool of strongly bound molecules. However, the rapid fall of residence time seen in native H1.4 upon core histone hyperacetylation is not seen in hybrid H1.1−1.4. H1 variant H1.5, which saw no change in residence time following core histone hyperacetylation, now sees a significant decline when coupled with the globular domain of H1.1.

This suggests that the NTD can make a subtle contribution to the influence of acetylation on histone H1 binding.

Hyperacetylation Changes the Cooperativity of H1 Binding to Chromatin. Recent evidence suggests that the contributions of the CTD and globular domains to histone H1 binding are more than just additive. The globular domain, which contains two defined DNA binding sites, only binds with one site in the absence of the CTD. In the presence of the CTD, both sites are engaged. The result is that the globular domain and the CTD bind to chromatin cooperatively (*65*). We therefore wished to test whether or not cooperativity was altered in the presence of histone acetylation. For the following cooperativity experiments, H1.1 was selected as a prototype for other H1 variants, given its midrange affinity to chromatin and similar amino acid length to H1.2 (213 AA compared to 215 AA in H1.1) and H1.4 (219 AA). Before we measured the change in cooperativity in the entire H1.1 molecule, we measured the binding affinities of the individual subdomains in the presence of hyperacetylation. We found that the globular domain and the CTD (of H1.1) by themselves failed to show a change in recovery following treatment with TSA (18 h) (Figure 6e,f). This is in contrast to the increase in effective diffusion and reduction of residence time seen when the domains are coupled (as in WT H1). We then compared the kinetics of the H1 molecule with key mutations in the individual sites of the globular domain. The globular domain consists of two sites, site I and site II, which are critical in binding to DNA (*64*). Site I is thought to bind DNA near the nucleosomal dyad, while site II is thought to interact with linker DNA. As has already been shown in msH1° (R42A site II and K73A site I), mutation of critical residues in these sites in H1.1 (R57A site II and K88A site I) also leads to significant change in recovery (Figure 6a). Note that these mutants still have an intact CTD. Interestingly, mutations at either site in the globular domain are enough to abrogate the response to core histone hyperacetylation (Figure 6b−d), with no effect on the effective diffusion coefficient being observed. The removal of the CTD (R57AΔCTD, R57AK88AΔCTD) did not alter the effective diffusion coefficient in the presence of hyperacetylation (data not shown).

These results suggest that the only way histone hyperacetylation may be able to impact H1 dynamics is by decreasing the cooperativity in binding to chromatin. Cooperativity in binding is present when the binding of one domain influences (in a positive or a negative manner) the binding of the other domain. A mathematical model for assessing cooperativity was recently described in ref *65*. The degree of cooperativity (γ) is proportional to the difference in the ratio of the bound and freely diffusing subpopulation in the complete protein (WT protein) and the sum of the ratios of the individual binding domains (*65*).

Since the individual domains (CTD, globular domain, sites I and II) do not change their kinetics upon hyperacetylation, the change in cooperativity ($\Delta\gamma$) is just proportional to the change in the ratio of bound to free WT H1 molecules upon hyperacetylation. A mathematical formula for measuring the change in cooperativity is given in the Supporting Information. If there is no change in cooperativity ($\Delta\gamma = 0$), then there is no change in how the two domains bind following the modification (i.e., hyperacetylation). On the other hand, if there were a negative change ($\Delta\gamma < 0$), then the binding of one domain would not support the binding of the other domain in the presence of the modification (i.e., hyperacetylation). Based on our calculations on the change in cooperativity, all H1 variants and hybrids undergo a negative change in cooperative binding upon hyperacetylation (Figure 7).

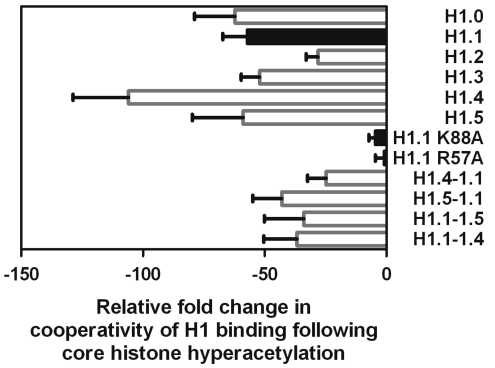

FIGURE 7: Cooperativity in H1 binding is reduced following hyperacetylation. The change in cooperativity ($\Delta\gamma$) is a function of the difference of the reciprocal product of the effective diffusion coefficient and the fraction that is effectively diffusing following hyperacetylation (provided the individual domains do not change their affinity). Based on this relation, H1.1 undergoes a 60-fold decrease in cooperativity, while H1.4 is predicted to have a 100-fold decrease in cooperative binding. Predicted values are shown in gray bars, while calculated values are shown in black.

As per the existing model of H1 binding to chromatin, the CTD establishes initial contact, followed by the cooperative binding of either site I or site II to DNA (*64*, *65*). Analyzing the change in recovery of the K88A mutant allowed us to assess the change in cooperation between the CTD and site II upon H1 binding, while the R57A mutant allowed us to assess the change in cooperation between the CTD and site I upon H1 binding. Since these two mutants suffer negligible changes to D_{eff} upon hyperacetylation, a change in cooperativity $\Delta\gamma \approx 0$ is seen (a value of -1 ± 4 for R57A and -4 ± 3 for K88A). This implies that the binding of the CTD−site I or CTD−site II is unaffected by hyperacetylation (Figure 8). However, when all of the three domains of H1 are present (site I, site II, and the CTD), there is a big change in the cooperativity of binding in the presence of hyperacetylation (Figure 7). This change therefore occurs during the transition of CTD−site I binding or CTD−site II binding to CTD−site I−site II binding, which eventually paves the way for high-affinity binding. H1.1 undergoes a change of cooperativity by a factor of −60 following hyperacetylation. Note that this decrease is relative to control cells, since the absolute change in cooperativity would depend upon the ratio of bound and free fractions of the individual binding domains of the molecule.

Extrapolating these calculations to other variants and hybrids of H1, we see that all of the variants and H1 hybrids show decreased cooperativity, with H1.4 having an almost 100-fold decrease in cooperativity when compared to control cells. This extrapolation is a predicted loss of cooperativity, since we did not directly measure the individual binding domains for other histone H1s. The validity of the extrapolation rests on the assumption that the individual binding domains of the variants, like H1.1, do not undergo a change in cooperativity and that the change is observed only in the intact molecule.

DISCUSSION

Core histone acetylation has been shown to modify the structure of the chromatin fiber (*66*−*69*). Biochemical evidence suggests that hyperacetylation causes a moderate loosening of

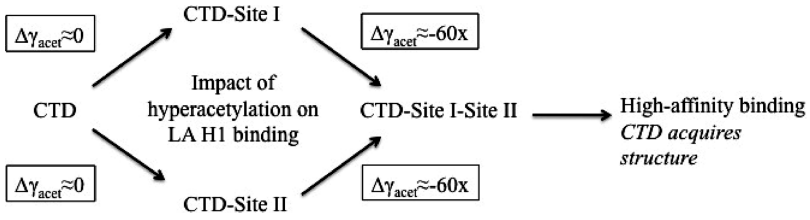

FIGURE 8: Impact of hyperacetylation on LA and HA sites. Following the initial interaction of the CTD, either site I or site II of the globular domain interacts with their respective binding sites. This step is not significantly affected by hyperacetylation, as judged by the response of R57A, K88A H1.1 mutants to hyperacetylation. The transition from this state to a state that allows all of the domains of H1 to be cooperatively bound is most affected by hyperacetylation (60-fold decease in H1.1). Once the three-dimensional structure of the CTD is acquired, hyperacetylation acts on decreasing either the residence time, transition time, or the proportion of strongly bound H1 molecules in a variant-specific manner.

chromatin (*45*, *70*). The loosening of chromatin is consistent with weaker DNA−histone interactions seen in the thermal denaturation profile and increased DNase I susceptibility of nucleosome particles following hyperacetylation (*71*). From these studies, it can be inferred that core histone acetylation should impact all histone H1 variants equally through the potential disruption of the histone H1 binding site on the surface of the nucleosome. Instead, on the basis of our results, we find significant differences in the relative change in cooperativity and the variant-specific changes in HA population. This suggests that either (a) disruption of the H1 binding site by acetylation is not the sole mechanism explaining the influence of acetylation on H1 binding or (b) different H1 subtypes have different requirements for binding to the surface of the nucleosome.

There have been previous attempts to address the influence of histone acetylation on the binding of H1 histones in living cells (*53*, *72*). Following a 2 h incubation with TSA, mouse H1.2 (H1c) and H1.0 (H1°) were found to have a significantly shorter residency time in both euchromatin and heterochromatin regions. We chose to examine cells after 1 h treatment with TSA and after 18 h treatment with TSA. This was chosen to preferentially reflect the separate kinetic pools of acetylated histones (reviewed in ref *73*). Brief periods of incubation with deacetylase inhibitors impact primarily euchromatic pools of histones while much longer incubations are required to impact heterochromatin regions. Surprisingly, the 1 h treatment with TSA had no significant impact on the recovery of histone H1 in euchromatin. This may be a reflection of the relatively low abundance of hyperacetylated chromatin in euchromatin. A 1 μm circle necessary for conducting the FRAP experiment may limit the sensitivity to detect these smaller pools of chromatin. The failure to alter the recovery in heterochromatin following a 1 h treatment with TSA was expected based on the slow kinetics of acetylation, even in the presence of TSA.

Induction of core histone hyperacetylation by longer treatments evoked marked changes in mobility of all H1 variants analyzed, with a consistent change in the effective diffusion coefficient being observed for all H1 variants tested. The effective diffusion coefficient reflects the combined contributions of both a small freely diffusing pool and a much larger weakly bound (LA) population that constitutes the bulk of the histone H1 nuclear pool for all variants. The increased effective diffusion coefficient can arise through two (or more) mutually inclusive mechanisms. The number of H1 binding sites may be reduced by disruption of chromatin structure and, in particular, the trajectory of the DNA at the entry and exit points of the nucleosome. This would result in an increase in the freely diffusing pool of H1. The other way effective diffusion coefficient can increase is if H1 is engaged in LA interactions and is unable to progress to HA interactions with chromatin. This implies that H1 cycles rapidly back and forth between freely diffusing and LA interactions upon hyperacetylation. This is almost certainly the case in this instance because the population of freely diffusing histone H1 is so small that these measurements are not sensitive enough to detect even a several-fold change in freely diffusing H1.

The changes imparted to the HA H1 population are more varied. Unexpectedly, the distribution of histone H1 between HA and LA sites is largely unchanged. The exception is histone H1.2, where the proportion of molecules bound to HA sites decreases by approximately 30%. Interestingly, H1.2 is also unique in that the transition time and the residence time in the HA sites are unchanged. Thus, for histone H1.2, the recycling at LA sites is increased but the duration of time it takes for an individual histone H1.2 molecule to convert to a HA site remains the same. Histone H1.2, commonly the most abundant histone H1 in the cell, may see a reduction in available binding sites as a result of changes in chromatin and nucleosome structure upon histone hyperacetylation.

The transition time reflects the duration that an individual histone H1 molecule spends cycling between LA binding sites and unbound diffusing states before engaging in a HA interaction that provides a relative immobilization of the histone H1 molecule. It reflects the likelihood that an interaction will be of high affinity. For H1.1 and H1.5 the transition time decreases. The increased cycling (the effective diffusion coefficient is increased) implies that the probability of engaging in a HA interaction may not have changed significantly for these two variants. For the remaining H1s, however, the transition time remains unchanged. With the increased cycling of these variants, this implies that the probability of either directly engaging or, more likely, converting from LA to HA binding is significantly lower following TSA treatment. Nonetheless, the proportion of binding sites that are HA remains the same.

The residence time is a measure of the binding affinity of histone H1 at sites where it binds with relatively high stability. For most H1 subtypes, the residence time of an H1 molecule at a high affinity site is dramatically reduced. This illustrates that hyperacetylation has a very significant effect on the ability of histone H1 to be retained at sites of high-affinity binding. The exceptions to this are H1.2 and H1.5. The binding of H1.5 seems remarkably robust in spite of hyperacetylation.

H1 binding to chromatin is largely mediated by the cooperative binding of the H1 CTD and globular domain (*65*). These individual domains do not alter their kinetics upon hyperacetylation. Since there is a dramatic effect when these individual domains are combined in the wild-type protein, we concluded that it is the cooperativity of binding that is impaired upon hyperacetylation. In the case of H1.1, acetylation led to decreased

cooperativity, and the primary indicator of this change was the effective diffusion coefficient. This implies that the transition from a state partially bound by two domains, either CTD−site I or CTD−site II, to a state bound by all three domains, CTD−site I−site II, is impaired (by a factor of 60× in H1.1 and a predicted value of 100× for H1.4). The latter state would pave the way for the acquisition of the three-dimensional structure of the CTD allowing for high-affinity binding. The transition to a state in which both globular domain sites and the CTD are bound occurs less frequently, leaving more H1 in LA and freely diffusing states. From a structural perspective, this implies that the CTD−site I or CTD−site II binding state is unable to undergo a conformational change that would bring the nucleosome entry and the exit linker DNA stems together, which is a prerequisite for high-affinity H1 binding and, indeed, higher order chromatin structure.

In conclusion, we have shown that core histone acetylation plays a pivotal role in regulating the dynamics of all histone H1 family members tested. However, once H1 binds to chromatin, the effect of core histone hyperacetylation becomes varied. It can affect the residence time, transition time, or the proportion of HA molecules in a variant-specific manner. In all cases, there is a significant reduction in the cooperativity of binding.

ACKNOWLEDGMENT

We thank Darin McDonald, Christi Andrin, and the Cell Imaging Facility, CCI, for technical assistance.

SUPPORTING INFORMATION AVAILABLE

Assessing change in cooperativity in H1 binding to chromatin (mathematical derivation), effect of TSA on histone acetylation, phosphorylation, etc., effect of Hoechst on H1 mobility, FRAP recovery profiles of H1 variants postinduction of core histone acetylation (TSA treatment for 1 h) enriched in euchromatin and heterochromatin, and FRAP recovery profiles of H1 variants postinduction of core histone acetylation (TSA treatment for 18 h) enriched in euchromatin and heterochromatin. This material is available free of charge via the Internet at http://pubs.acs.org.

REFERENCES

1. Widom, J. (1998) Structure, dynamics, and function of chromatin in vitro. *Annu. Rev. Biophys. Biomol. Struct. 27*, 285.
2. Ramakrishnan, V. (1997) Histone H1 and chromatin higher-order structure. *Crit. Rev. Eukaryot. Gene Expression 7*, 215.
3. Zlatanova, J., and van Holde, K. (1996) The linker histones and chromatin structure: new twists. *Prog. Nucleic Acid Res. Mol. Biol. 52*, 217–259.
4. van Holde, K., and Zlatanova, J. (1996) What determines the folding of the chromatin fiber? *Proc. Natl. Acad. Sci. U.S.A. 93*, 10548–10555.
5. Thoma, F. (1979) Involvement of histone H1 in the organization of the nucleosome and of the salt-dependent superstructures of chromatin. *J. Cell Biol. 83*, 403–427.
6. Lennox, R. W., and Cohen, L. H. (1983) The histone H1 complements of dividing and nondividing cells of the mouse. *J. Biol. Chem. 258*, 262–268.
7. D'Incalci, M., Allavena, P., Wu, R. S., and Bonner, W. M. (1986) H 1 variant synthesis in proliferating and quiescent human cells. *Eur. J. Biochem. 154*, 273–279.
8. Kinkade, J. M., Jr., and Cole, R. D. (1966) The resolution of four lysine-rich histones derived from calf thymus. *J. Biol. Chem. 241*, 5790.
9. Pehrson, J. R., and Cole, R. D. (1982) Histone H1 subfractions and H10 turnover at different rates in nondividing cells. *Biochemistry 21*, 456–460.
10. Khochbin, S., and Wolffe, A. P. (1994) Developmentally regulated expression of linker-histone variants in vertebrates. *FEBS J. 225*, 501–510.
11. Higurashi, M., Adachi, H., and Ohba, Y. (1987) Synthesis and degradation of H1 histone subtypes in mouse lymphoma L5178Y cells. *J. Biol. Chem. 262*, 13075–13080.
12. Liao, L. W., and Cole, R. D. (1981) Condensation of dinucleosomes by individual subfractions of H1 histone. *J. Biol. Chem. 256*, 10124–10128.
13. Liao, L. W., and Cole, R. D. (1981) Differences among H1 histone subfractions in binding to linear and superhelical DNA. Sedimentation velocity studies. *J. Biol. Chem. 256*, 11145–11150.
14. Nagaraja, S., Delcuve, G. P., and Davie, J. R. (1995) Differential compaction of transcriptionally competent and repressed chromatin reconstituted with histone H1 subtypes. *Biochim. Biophys. Acta 1260*, 207–214.
15. Khadake, J. R., and Rao, M. R. S. (1995) DNA- and chromatin-condensing properties of rat testes H1a and H1t compared to those of rat liver H1bdec: H1t is a poor condenser of chromatin. *Biochemistry 34*, 15792–15801.
16. Th'ng, J. P., Sung, R., Ye, M., and Hendzel, M. J. (2005) H1 family histones in the nucleus. Control of binding and localization by the C-terminal domain. *J. Biol. Chem. 280*, 27809.
17. Kornberg, R. D., and Lorch, Y. (1999) Twenty-five years of the nucleosome, review fundamental particle of the eukaryote chromosome. *Cell 98*, 285.
18. Strahl, B. D., and Allis, C. D. (2000) The language of covalent histone modifications. *Nature 403*, 41.
19. Wolffe, A. P., and Kurumizaka, H. (1998) The nucleosome: a powerful regulator of transcription. *Prog. Nucleic Acid Res. Mol. Biol. 61*, 379.
20. Wolffe, A. P., and Hayes, J. J. (1999) Chromatin disruption and modification. *Nucleic Acids Res. 27*, 711.
21. Wu, C. (1997) Chromatin remodeling and the control of gene expression. *J. Biol. Chem. 272*, 28171.
22. Schlissel, M. S., and Brown, D. D. (1984) The transcriptional regulation of *Xenopus* 5S RNA genes in chromatin: the roles of active stable transcription complexes and histone H1. *Cell 37*, 903–913.
23. Laybourn, P. J., and Kadonaga, J. T. (1991) Role of nucleosomal cores and histone H1 in regulation of transcription by RNA polymerase II. *Science 254*, 238.
24. Thomas, J. O. (1999) Histone H1: location and role. *Curr. Opin. Cell Biol. 11*, 312.
25. Zlatanova, J., and Van Holde, K. (1992) Histone H1 and transcription: still an enigma? *J. Cell Sci. 103* (Part 4), 889.
26. Folco, H. D., Freitag, M., Ramon, A., Temporini, E. D., Alvarez, M. E., Garcia, I., Scazzocchio, C., Selker, E. U., and Rosa, A. L. (2003) Histone H1 is required for proper regulation of pyruvate decarboxylase gene expression in *Neurospora crassa*. *Eukaryot. Cell 2*, 341–350.
27. Koop, R., Di Croce, L., and Beato, M. (2003) Histone H1 enhances synergistic activation of the MMTV promoter in chromatin. *EMBO J. 22*, 588.
28. Takami, Y., Nishi, R., and Nakayama, T. (2000) Histone H1 variants play individual roles in transcription regulation in the DT40 chicken B cell line. *Biochem. Biophys. Res. Commun. 268*, 501–508.
29. Crane-Robinson, C. (1999) How do linker histones mediate differential gene expression? *BioEssays 21*, 367–371.
30. Wolffe, A. P., Khochbin, S., and Dimitrov, S. (1997) What do linker histones do in chromatin? *BioEssays 19*, 249.
31. Shen, X., and Gorovsky, M. A. (1996) Linker histone H1 regulates specific gene expression but not global transcription in vivo. *Cell 86*, 475.
32. Fan, Y., Nikitina, T., Zhao, J., Fleury, T. J., Bhattacharyya, R., Bouhassira, E. E., Stein, A., Woodcock, C. L., and Skoultchi, A. I. (2005) Histone H1 depletion in mammals alters global chromatin structure but causes specific changes in gene regulation. *Cell 123*, 1199.
33. Fan, Y., Nikitina, T., Morin-Kensicki, E. M., Zhao, J., Magnuson, T. R., Woodcock, C. L., and Skoultchi, A. I. (2003) H1 linker histones are essential for mouse development and affect nucleosome spacing in vivo. *Mol. Cell. Biol. 23*, 4559–4572.
34. Perry, C. A., and Annunziato, A. T. (1989) Influence of histone acetylation on the solubility, H1 content and DNase I sensitivity of newly assembled chromatin. *Nucleic Acids Res. 17*, 4275.
35. Perry, C. A., and Annunziato, A. T. (1991) Histone acetylation reduces H1-mediated nucleosome interactions during chromatin assembly. *Exp. Cell Res. 196*, 337.
36. Hebbes, T. R., Clayton, A. L., Thorne, A. W., and Crane-Robinson, C. (1994) Core histone hyperacetylation co-maps with generalized DNase I sensitivity in the chicken β-globin chromosomal domain. *EMBO J. 13*, 1823–1830.
37. Struhl, K. (1998) Histone acetylation and transcriptional regulatory mechanisms. *Genes Dev. 12*, 599–606.
38. Reeves, R. (1984) Transcriptionally active chromatin. *Biochim. Biophys. Acta 782*, 343–393.

39. Vidali, G., Ferrari, N., and Pfeffer, U. (1988) Histone acetylation: a step in gene activation. *Adv. Exp. Med. Biol. 231*, 583–596.
40. Loidl, P. (1988) Towards an understanding of the biological function of histone acetylation. *FEBS Lett. 227*, 91.
41. Hebbes, T. R., Thorne, A. W., and Crane-Robinson, C. (1988) A direct link between core histone acetylation and transcriptionally active chromatin. *EMBO J. 7*, 1395–1402.
42. Roth, S. Y., Denu, J. M., and Allis, C. D. (2001) Histone acetyltransferases. *Annu. Rev. Biochem. 70*, 81–120.
43. Taunton, J., Hassig, C. A., and Schreiber, S. L. (1996) A mammalian histone deacetylase related to the yeast transcriptional regulator Rpd3p. *Science 272*, 408.
44. Shahbazian, M. D., and Grunstein, M. (2007) Functions of site-specific histone acetylation and deacetylation. *Annu. Rev. Biochem. 76*, 75–100.
45. Annunziato, A. T., Frado, L. L., Seale, R. L., and Woodcock, C. L. (1988) Treatment with sodium butyrate inhibits the complete condensation of interphase chromatin. *Chromosoma 96*, 132–138.
46. Tse, C., Sera, T., Wolffe, A. P., and Hansen, J. C. (1998) Disruption of higher-order folding by core histone acetylation dramatically enhances transcription of nucleosomal arrays by RNA polymerase III. *Mol. Cell. Biol. 18*, 4629–4638.
47. Wang, X., and Hayes, J. J. (2008) Acetylation mimics within individual core histone tail domains indicate distinct roles in regulating the stability of higher-order chromatin structure. *Mol. Cell. Biol. 28*, 227–236.
48. Shogren-Knaak, M., Ishii, H., Sun, J. M., Pazin, M. J., Davie, J. R., and Peterson, C. L. (2006) Histone H4-K16 acetylation controls chromatin structure and protein interactions. *Science 311*, 844–847.
49. Robinson, P. J., and Rhodes, D. (2006) Structure of the "30 nm" chromatin fibre: a key role for the linker histone. *Curr. Opin. Struct. Biol. 16*, 336–343.
50. Hendzel, M. J., Lever, M. A., Crawford, E., and Th'ng, J. P. (2004) The C-terminal domain is the primary determinant of histone H1 binding to chromatin in vivo. *J. Biol. Chem. 279*, 20028.
51. Raghuram, N., Carrero, G., Th'ng, J., and Hendzel, M. J. (2009) Molecular dynamics of histone H1. *Biochem. Cell Biol. 87*, 189–206.
52. Carrero, G., Crawford, E., Hendzel, M. J., and de Vries, G. (2004) Characterizing fluorescence recovery curves for nuclear proteins undergoing binding events. *Bull. Math. Biol. 66*, 1515–1545.
53. Misteli, T., Gunjan, A., Hock, R., Bustin, M., and Brown, D. T. (2000) Dynamic binding of histone H1 to chromatin in living cells. *Nature 408*, 877.
54. Shechter, D., Dormann, H. L., Allis, C. D., and Hake, S. B. (2007) Extraction, purification and analysis of histones. *Nat. Protoc. 2*, 1445–1457.
55. Yoshida, M., Kijima, M., Akita, M., and Beppu, T. (1990) Potent and specific inhibition of mammalian histone deacetylase both in vivo and in vitro by trichostatin A. *J. Biol. Chem. 265*, 17174–17179.
56. Panyim, S., and Chalkley, R. (1969) High resolution acrylamide gel electrophoresis of histones. *Arch. Biochem. Biophys. 130*, 337–346.
57. Carrero, G., Crawford, E., Th'ng, J., de Vries, G., and Hendzel, M. J. (2004) Quantification of protein-protein and protein-DNA interactions in vivo, using fluorescence recovery after photobleaching. *Methods Enzymol. 375*, 415.
58. Thevenaz, P., Ruttimann, U. E., and Unser, M. (1998) A pyramid approach to subpixel registration based on intensity. *IEEE Trans. Image Process 7*, 27–41.
59. Carrero, G., Raghuram, N., Th'ng, J., and Hendzel, M. (2009) A method for assessing kinetic changes of histone H1 after post-translational modifications. *AIP Conf. Proc. 1168 2*, 1306–1309.
60. Kim, Y., Yoshida, M., and Horinouchi, S. (1999) Selective induction of cyclin-dependent kinase inhibitors and their roles in cell cycle arrest caused by trichostatin A, an inhibitor of histone deacetylase. *Ann. N.Y. Acad. Sci. 886*, 200–203.
61. Carrero, G., McDonald, D., Crawford, E., de Vries, G., and Hendzel, M. J. (2003) Using FRAP and mathematical modeling to determine the in vivo kinetics of nuclear proteins. *Methods 29*, 14–28.
62. Parseghian, M. H., and Hamkalo, B. A. (2001) A compendium of the histone H1 family of somatic subtypes: an elusive cast of characters and their characteristics. *Biochem. Cell Biol. 79*, 289.
63. Parseghian, M. H., Newcomb, R. L., Winokur, S. T., and Hamkalo, B. A. (2000) The distribution of somatic H1 subtypes is non-random on active vs. inactive chromatin: distribution in human fetal fibroblasts. *Chromosome Res. 8*, 405.
64. Brown, D. T., Izard, T., and Misteli, T. (2006) Mapping the interaction surface of linker histone H1(0) with the nucleosome of native chromatin in vivo. *Nat. Struct. Mol. Biol. 13*, 250–255.
65. Stasevich, T. J., Mueller, F., Brown, D. T., and McNally, J. G. (2010) Dissecting the binding mechanism of the linker histone in live cells: an integrated FRAP analysis, EMBO J. (in press).
66. Fletcher, T. M., and Hansen, J. C. (1995) Core histone tail domains mediate oligonucleosome folding and nucleosomal DNA organization through distinct molecular mechanisms. *J. Biol. Chem. 270*, 25359–25362.
67. Garcia-Ramirez, M., Rocchini, C., and Ausio, J. (1995) Modulation of chromatin folding by histone acetylation. *J. Biol. Chem. 270*, 17923–17928.
68. Wang, X., He, C., Moore, S. C., and Ausio, J. (2001) Effects of histone acetylation on the solubility and folding of the chromatin fiber. *J. Biol. Chem. 276*, 12764–12768.
69. Carruthers, L. M., and Hansen, J. C. (2000) The core histone N termini function independently of linker histones during chromatin condensation. *J. Biol. Chem. 275*, 37285–37290.
70. McGhee, J. D., Nickol, J. M., Felsenfeld, G., and Rau, D. C. (1983) Histone hyperacetylation has little effect on the higher order folding of chromatin. *Nucleic Acids Res. 11*, 4065–4075.
71. Ausio, J., and van Holde, K. E. (1986) Histone hyperacetylation: its effects on nucleosome conformation and stability. *Biochemistry 25*, 1421–1428.
72. Rao, J., Bhattacharya, D., Banerjee, B., Sarin, A., and Shivashankar, G. V. (2007) Trichostatin-A induces differential changes in histone protein dynamics and expression in HeLa cells. *Biochem. Biophys. Res. Commun. 363*, 263–268.
73. Davie, J. R., and Hendzel, M. J. (1994) Multiple functions of dynamic histone acetylation. *J. Cell. Biochem. 55*, 98–105.